Supporting Information

Ultrathin 2D-2D NiFe LDH/MOF heterojunction nanosheets: an efficient oxygen evolution reaction catalyst for water oxidation†

Haoran Yin,‡[a] Shibiao Su,‡[a] Di Yao,‡[a] Lixia Wang,[a] Xinqiang Liu,[a] Tayirjan Taylor Isimjan,[c] Xiulin Yang,*[a] Dandan Cai*[a,b]

[a] *Guangxi Key Laboratory of Low Carbon Energy Materials, School of Chemistry and Pharmaceutical Sciences, Guangxi Normal University, Guilin 541004, P.R. China*

[b] *School of Chemical Engineering and Technology, Sun Yat-sen University, Zhuhai 519082, P.R. China*

[c] *Saudi Arabia Basic Industries Corporation (SABIC) at King Abdullah University of Science and Technology (KAUST), Thuwal 23955-6900, Saudi Arabia*

[1] These authors contribute equally to this work.

* Corresponding authors: caidandan86@163.com, xlyang@gxnu.edu.cn

List of Contents

1. Experimental

Materials

The reagents were supplied by the supplier without purification. Naphthalene-2,6-dicarboxylic acid (NDA, $C_{12}H_8O_4$, 98%), nickel (II) chloride hexahydrate ($NiCl_2 \cdot 6H_2O$, 98%), ferric chloride hexahydrate ($FeCl_3 \cdot 6H_2O$, 99%), urea (H_2NCONH_2, 99%), ammonium fluoride (NH_4F, 98%), and potassium hydroxide (KOH, 90%) were purchased from Aladdin Chemical Reagent Co. Ltd. Absolute ethanol (EtOH, 99.7%) and N, N-dimethylformamide (DMF, 98%) were purchased from Xilong Chemical Reagent Co. Ltd. The carbon fiber paper (CP) purchased from Toray Co. Ltd. and was utilized with a dimension of 2 cm ×1 cm in the experiments. Commercial Pt/C (20 wt.% Pt) and Nafion solution (5 wt.%) were purchased from Alfa Aesar. The RuO_2 was prepared by directly pyrolysis of $RuCl_3$ in air at 400 °C and $RuCl_3 \cdot 3H_2O$ (37%) were purchased from Inno-chem.

Treatment of CP

The surface of the CP was hydrothermally treated by 68% HNO_3 at 120 °C for 180 min, and then cleaned with deionized water and absolute ethanol.

Synthesis of NiFe LDH

Firstly, $NiCl_2 \cdot 6H_2O$ (0.9 mmol), $FeCl_3 \cdot 6H_2O$ (0.3 mmol), urea (8.3 mmol) and NH_4F (8.3 mmol) were dispersed in deionized water (20 mL) to form a clear solution. The resulting solution was then transferred to a 25 mL Taflon-lined stainless-steel autoclave with two pieces of modified CP. The autoclave was sealed at 120 °C and maintained for 16 h. After cooling to room temperature, the targeted NiFe LDH catalyst was taken out and washed three times with anhydrous ethanol, then dried at 60 ℃ for 8 h.

Synthesis of NiFe LDH/MOF and NiFe MOF

The obtained NiFe LDH was dipped in a 4.5 mL mixed solution consisting of 50 mg NDA, 4 mL DMF, and 0.5 mL deionized water. Then, a hydrothermal reaction was carried out at 120 °C in a PTFE reactor for 24 h. Finally, the resulting NiFe LDH/MOF was taken out, washed three times with absolute ethanol, and dried at 60 ℃ for 8 h. Besides, NiFe MOF was synthesized using a similar method to NiFe LDH/MOF, except for a reaction time of 48 h.

Synthesis of RuO_2/CP and Pt/C/CP

For comparison, RuO_2 and Pt/C on CP were also prepared. A homogeneous catalyst ink is formed by dispersing 2 mg RuO_2 or Pt/C in 250 μL deionized water/isopropyl alcohol (V/V =

1:1) and 25 μL 5% Nafion as a binder. The mixture is then dropped on the surface of the CP (1 cm × 0.5 cm) and dried in indoor environment.

2. Characterization

The structure of samples was detected by a powder X-ray diffractometer (PXRD, Rigaku D/Max-3c, Cu-Kα radiation, λ = 1.54056 Å). The morphologies and compositions of samples were investigated by scanning electron microscopy (SEM, Gemini Sigma 300) and transmission electron microscopy (TEM, Talos F200S, TFS, USA) equipped with Rontec energy-dispersive X-ray system (EDS) and selected area electron diffraction (SAED). The nanosheets thicknesses of the samples were evaluated by atomic force microscope (AFM; Dimension ICON, Bruker, America). The atomic composition and valence states of the samples were measured by employing the X-ray photoelectron spectroscopy (XPS, ESCA-LAB250, Al Kα excitation source at 1486.6 eV). The functional groups of samples were analyzed by Fourier-transform infrared spectroscopy (FT-IR; Spectrum Two, PerkinElmer). Raman spectra of samples were obtained by in Via Quotation Evolution (Renishaw, 514 nm laser sourc).

3. Electrochemical measurements

Electrochemical measurements were conducted using the CHI760E electrochemical workstation (Chenhua Instrument, Shanghai, China) with a standard three-electrode system (The as-synthesized catalyst was acted as integrated working electrode, carbon rod and Hg/HgO were used as the counter electrode and the reference electrode, respectively) in 1.0 M KOH aqueous solution. All electrode potentials were converted to reversible hydrogen electrode (RHE) electrode potentials by the Nernst equation: $E_{vs.\ RHE} = E_{vs.\ Hg/HgO} + 0.059pH + 0.098$ V. The oxygen evolution overpotential (η) was calculated according to the following formula: $\eta\ (V) = E_{vs.\ RHE} - 1.23$ V. Linear sweep voltammetry (LSV) was performed at a scan rate of 1 mV s^{-1} from 1.2V to 0.3 V. All LSV polarization curves were corrected using 95% *iR* compensation. The Tafel slope was plotted by converting the LSV curve according to the following formula: $\eta = a + b \log j$, where η was the overpotential (mV), j was the corresponding current density (mA cm^{-2}), b was the Tafel slope (mV dec^{-1}). CV tests were performed at different sweep rates in the non-Faraday region (0.9 – 1.0 V) to estimate the electrochemical double layer capacitance (C_{dl}). The C_{dl} was calculated by the equation: $C_{dl} = (j_a - j_c)/ (2\times\nu)$, where j_a, j_c and ν corresponds to the current density of anode and cathode, and scan rate, respectively. Electrochemical ac impedance (EIS) was performed in the frequency range 10,000 Hz - 0.01 kHz with an amplitude of 5 mV. The stabilities were assessed by cyclic voltammetry (CV, 0.3–0.9 V, 0.1 V s^{-1}), chronopotentiometry (CP, no *iR* compensation, constant current density of 10 mA cm^{-2}) and

multi-step chronopotentiometry (ISTEP, no *iR* compensation) to the stability of the active electrode.

The value of TOF is calculated according to the following formula:

$$\mathrm{TOF} = \frac{j\mathrm{A}}{4\mathrm{nF}}$$

Here, A (cm^2) represents the geometric area of the CFP. The number 4 means the four electrons transfer in OER and F is equal to the constant of 96485.3 C mol^{-1}. n represents the number of mole metal ions in the samples.

4. Electrochemical in-situ Raman spectra measurements

The in-situ Raman spectroscopy experiments were performed using a Raman spectrometer (InVia Qontor, Renishaw) equipped with an in-situ test electrolytic cell (Gaoss Union C031-1). The laser excitation wavelength used was 532 nm and the exposure time was set to 10 min for each spectrum. The as-prepared catalyst, carbon rod and Ag/AgCl electrode were served as the working electrode, counter electrode and reference electrode, respectively. The evolution of catalyst was monitored by gathering Raman spectra at constant potential ranging from 1.1 to 1.5 V (vs. RHE).

5. Supplementary Figures

Fig. S1. FT-IR spectra of NiFe LDH, NiFe LDH/MOF, NiFe MOF and NDA organic ligands.

Fig. S2. Cyclic voltammograms (CVs) curves in the non-Faradaic potential range at different scan rates (5 - 30 mV s^{-1}) of (a) NiFe LDH, (b) NiFe LDH/MOF, (c) NiFe MOF, (d) Corresponding C_{dl} values of NiFe LDH, NiFe LDH/MOF and NiFe MOF.

Fig. S3. Raman spectra of NiFe LDH/MOF after stability test.

6. Supplementary Tables

Table S1. The true content of metal elements in different catalysts obtained by ICP-MS measurements.

Table S2. Summary of previously reported excellent OER catalysts in alkaline solution.

Table S3. Comparison of the overall-water-splitting activities among various recently reported electrocatalysts tested in 1.0 M KOH.

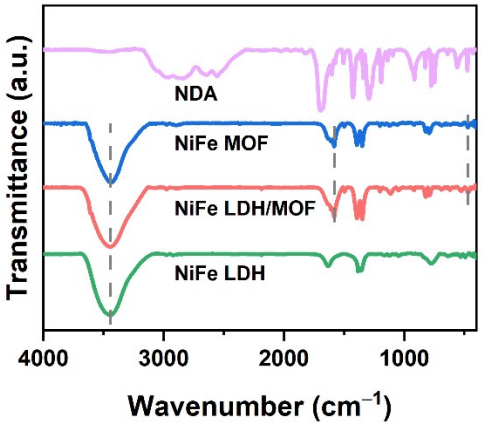

Fig. S1. FT-IR spectra of NiFe LDH, NiFe LDH/MOF, NiFe MOF and NDA organic ligands.

The formation of NiFe LDH, NiFe LDH/MOF, and NiFe MOF was further substantiated by the fourier transform infrared spectroscopy (FT-IR). For comparison, the IR spectrum of pure NDA also be investigated, which is consistent with the previously reported.[1] The absorption spectrum peaks at approximately 3450 cm^{-1} and 1630 cm^{-1} can be attributed to O-H stretching vibration and H-O-H bending vibration of the absorbent water in NiFe LDH, respectively.[2] And the peak at about 1358 cm^{-1} can be ascribed to the CO_3^{2-} vibrations, while the peaks below 1000 cm^{-1} correspond to M-O vibrations.[3] Meanwhile, the characteristic peaks at 1585 cm^{-1} and 471 cm^{-1} in NiFe LDH/MOF and NiFe MOF can be assigned to the V_{as}(-COO-) and M-O vibrations of MOF, confirming that MOF is successfully anchored on LDH surfaces.[4] Interestingly, the weakened peak of NiFe LDH in NiFe LDH/MOF may be attributed to the lower content of NiFe LDH, which is consistent with the previously proposed dissolution-crystallization mechanism. These results clearly demonstrated the formation of NiFe LDH, NiFe LDH/MOF and NiFe MOF.

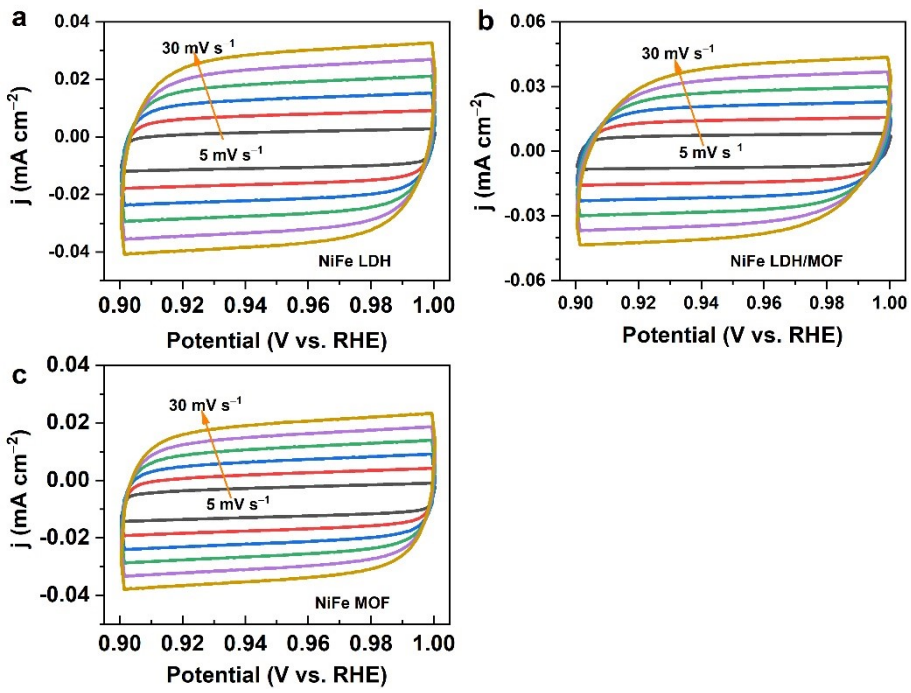

Fig. S2. Cyclic voltammograms (CVs) curves in the non-Faradaic potential range at different scan rates (5 - 30 mV s^{-1}) of (a) NiFe LDH, (b) NiFe LDH/MOF, (c) NiFe MOF, and (d) corresponding C_{dl} values of NiFe LDH, NiFe LDH/MOF and NiFe MOF.

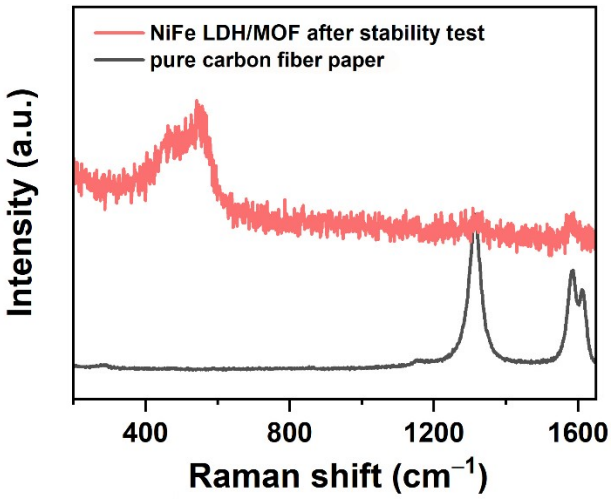

Fig. S3. Raman spectra of NiFe LDH/MOF after stability test.

Table S1. The true content of metal elements in different catalysts obtained by ICP-MS measurements.

Catalyst	Ni (wt%)	Fe (wt%)
NiFe LDH	30.8	47.2
NiFe LDH/MOF	30.6	45.3
NiFe MOF	25.3	42.6

Table S2. Summary of previously reported excellent OER catalysts in alkaline solution.

Catalyst	η_{10} (mV)	Tafel slope (mV dec^{-1})	Reference
NiFe LDH/MOF	**196**	**32.5**	**This work**
NiCo LDH@NiFe-MIL	270	75.1	[5]
NiCoCu LDH	224	78	[6]
$NiCo_2O_4$@NiFe-LDH	231	59	[7]
$CoMn_{0.01}$	255	66	[8]
FeNi MOF-CNTs	220	70.95	[9]
NiCo-NR	244	85	[10]
M-NiA-CoN	180	41	[11]
Ru@CoFe-LDH	249	50	[12]
CoNi-MOF	215	51.6	[13]
Ni_3Se_2@NiFe-LDH	220	61.3	[14]
$Er_{0.4}$Fe-MOF	210	73	[15]
Ni-MOF-74/N_3Ni	222	57	[16]

Table S3. Comparison of the overall-water-splitting activities among various recently reported electrocatalysts tested in 1.0 M KOH.

Catalyst (Cathode)	Catalyst (Anode)	Potential (V) at 10 mA cm^{-2}	Reference
NiFe LDH/MOF	**Pt/C**	**1.47**	**This work**
NFN-MOF/NF	NFN-MOF/NF	1.56	[17]
CoNiRu-NT	CoNiRu-NT	1.47	[18]
Co-NC@Ni_2Fe-LDH	Co-NC@Ni_2Fe-LDH	1.55	[19]
CoMoP,	CoMoP,	1.56	[20]
Ni-250-2@NF	Ni-250-2@NF	1.58	[21]
IrO_2@Ir-MOF	IrO_2@Ir-MOF	1.53	[22]
Co/CoP/NC	Co/CoP/NC	1.56	[21]
Ir@Ni-NDC	Ir@Ni-NDC	1.59	[23]
Ce@NiFe-MOF	Pt/C	1.56	[24]
Pt@LDH	Pt@LDH	1.49	[25]

References

1. J. Liu, J. Zhou, S. Liu, G. Chen, W. Wu, Y. li, P. Jin and C. Xu, Amorphous NiFe-layered double hydroxides nanosheets for oxygen evolution reaction, *Electrochim. Acta* 2020, **356**, 136827.
2. Y. Lin, H. Wang, C. K. Peng, L. Bu, C. L. Chiang, K. Tian, Y. Zhao, J. Zhao, Y. G. Lin, J. M. Lee and L. Gao, Co-Induced Electronic Optimization of Hierarchical NiFe LDH for Oxygen Evolution, *Small*, 2020, **16**, 2002426.
3. D. Tyndall, M. J. Craig, L. Gannon, C. McGuinness, N. McEvoy, A. Roy, M. Garcia-Melchor, M. P. Browne and V. Nicolosi, Demonstrating the source of inherent instability in NiFe LDH-based OER electrocatalysts, *J. Mater. Chem. A*, 2023, **11**, 4067-4077.
4. J. Jia, L. Wei, F. Li, C. Yu, K. Yang and T. Liang, In situ growth of NiFe MOF/NF by controlling solvent mixtures as efficient electrocatalyst in oxygen evolution, *Inorg. Chem. Commun.*, 2021, **128**, 108605.
5. L. Yang, L. Jin, K. Wang, H. Xu, G. He and H. Chen, Interface coupling induced built-in electric fields boost electrocatalytic oxygen evolution reaction over MOF@LDHs core-shell nanocones, *Colloids Surf. A Physicochem. Eng. Aspects.*, 2023, **672**, 131720.
6. A. Raja, N. Son, Y. I. Kim and M. Kang, Hybrid ternary NiCoCu layered double hydroxide electrocatalyst for alkaline hydrogen and oxygen evolution reaction, *J. Colloid Interface Sci.*, 2023, **647**, 104-114.
7. Z. Hu, S. Dong, Q. He, Z. Chen and D. Yuan, Synergetic Nanostructure Engineering and Electronic Modulation of a 3D Hollow Heterostructured $NiCo_2O_4$@NiFe-LDH Self-Supporting Electrode for Rechargeable Zn-Air Batteries, *Inorg. Chem.*, 2023, **62**, 7471-7482.

8. H. Zhang, N. Sun, X. Si, Y. Zhang, F. Ding, X. Kong and Y. Sun, Regulating the Electronic Structure of Metal-Organic Frameworks by Introducing Mn for Enhanced Oxygen Evolution Activity, *Inorg. Chem.*, 2024, **63**, 2997-3004.
9. L. Yaqoob, T. Noor, N. Iqbal, H. Nasir, N. Zaman and K. Talha, Electrochemical synergies of Fe–Ni bimetallic MOF CNTs catalyst for OER in water splitting, *J. Alloys Compd.*, 2021, **850**, 156583.
10. A. Gaur, V. Pundir, R. Kaur, S. N. Jha and V. Bagchi, Curtailing the Excess eg-Orbital Filling of a Ni Atom by Enhanced Interatomic Charge Transfer within a Bimetallic 2D Metal–Organic Framework for the Oxygen Evolution Reaction, *ACS Appl. Energy Mater.*, 2023, **6**, 5360-5367.
11. W. Zhang, M. Niu, J. Yu, S. Li, Y. Wang and K. Zhou, Mechanochemical Post-Synthesis of Metal–Organic Framework-Based Pre-Electrocatalysts with Surface Fe-O-Ni/Co Bonding for Highly Efficient Oxygen Evolution, *Adv. Funct. Mater.*, 2023, **33**, 2302014.
12. A. Karmakar, R. Jayan, A. Das, A. Kalloorkal, M. M. Islam and S. Kundu, Regulating Surface Charge by Embedding Ru Nanoparticles over 2D Hydroxides toward Water Oxidation, *ACS Appl. Mater. Interfaces*, 2023, **15**, 26928–26938.
13. L. Huang, G. Gao, H. Zhang, J. Chen, Y. Fang and S. Dong, Self-dissociation-assembly of ultrathin metal-organic framework nanosheet arrays for efficient oxygen evolution, *Nano Energy*, 2020, **68**, 104296.
14. J. Hu, S. Zhu, Y. Liang, S. Wu, Z. Li, S. Luo and Z. Cui, Self-supported Ni_3Se_2@NiFe layered double hydroxide bifunctional electrocatalyst for overall water splitting, *J. Colloid Interface Sci.*, 2021, **587**, 79-89.
15. Y. Ma, Y. Miao, G. Mu, D. Lin, C. Xu, W. Zeng and F. Xie, Highly Enhanced OER Performance by Er-Doped Fe-MOF Nanoarray at Large Current Densities, *Nanomaterials*, 2021, **11**, 1847.
16. N. Y. Hongnan Jia, Juan Zhu,Yujia Liu,Yunhao Lao,Hengjiang Cong,and Wei Luo, Ni_3N Modified MOF Heterostructure with Tailored Electronic Structure for Efficient Overall Water Splitting, *Chin. J. Struct. Chem.*, 2022, **41**, 2208031-2208036.
17. D. Senthil Raja, X.-F. Chuah and S.-Y. Lu, In Situ Grown Bimetallic MOF-Based Composite as Highly Efficient Bifunctional Electrocatalyst for Overall Water Splitting with Ultrastability at High Current Densities, *Adv. Energy Mater.*, 2018, **8**, 1801065.
18. Y. Wang, S. Wang, Z. L. Ma, L. T. Yan, X. B. Zhao, Y. Y. Xue, J. M. Huo, X. Yuan, S. N. Li and Q. G. Zhai, Competitive Coordination-Oriented Monodispersed Ruthenium Sites in Conductive MOF/LDH Hetero-Nanotree Catalysts for Efficient Overall Water Splitting in Alkaline Media, *Adv. Mater.*, 2022, **34**, 2107488.
19. T. Guo, L. Chen, Y. Li and K. Shen, Controllable Synthesis of Ultrathin Defect-Rich LDH Nanoarrays Coupled with MOF-Derived Co-NC Microarrays for Efficient Overall Water Splitting, *Small*, 2022, **18**, 2107739.
20. X. Wang, L. Yang, C. Xing, X. Han, R. Du, R. He, P. Guardia, J. Arbiol and A. Cabot, MOF-Derived Ultrathin Cobalt Molybdenum Phosphide Nanosheets for Efficient Electrochemical Overall Water Splitting, *Nanomaterials*, 2022, **12**, 1098.
21. S. Wang, Y. Zhang, X. Deng, Z. Ma, R. Cheng, Z. Wan, J. Li and X. Wang, Rational construction of loosely packed nickel nanoparticulates with residual HCOO ligands derived from a Ni-MOF for high-efficiency electrocatalytic overall water splitting, *J. Mater. Chem. A.*, 2023, **11**, 5222-5232.
22. L. Li, G. Li, Y. Zhang, W. Ouyang, H. Zhang, F. Dong, X. Gao and Z. Lin, Fabricating nano-

IrO_2@amorphous Ir-MOF composites for efficient overall water splitting: a one-pot solvothermal approach, *J. Mater. Chem. A.*, 2020, **8**, 25687-25695.

23. J. Yang, Y. Shen, Y. Sun, J. Xian, Y. Long and G. Li, Ir Nanoparticles Anchored on Metal-Organic Frameworks for Efficient Overall Water Splitting under pH-Universal Conditions, *Angew. Chem. Int. Ed.*, 2023, **62**, 202302220.
24. X. Wei, D. Liu, C. Wang, R. Yu, K. Zhang, S. Li, Z. Wu and Y. Du, Ce-Modified Flowerlike NiFe-MOF Nanostructure Based on Ion Competitive Coordination for Enhancing the Oxygen Evolution Reaction, *Inorg. Chem.*, 2023, **62**, 3238-3247.
25. J. M. Huo, Z. L. Ma, Y. Wang, Y. J. Cao, Y. C. Jiang, S. N. Li, Y. Chen, M. C. Hu and Q. G. Zhai, Monodispersed Pt Sites Supported on NiFe-LDH from Synchronous Anchoring and Reduction for High Efficiency Overall Water Splitting, *Small*, 2023, **19**, 2207044.